



Delft University of Technology

Wave Controls on Deltaic Shoreline-Channel Morphodynamics: Insights From a Coupled Model

Gao, Weilun; Nienhuis, Jaap; Nardin, William; Wang, Zhengbing ; Shao, Dongdong; Sun, Tao; Cui, Baoshan

DOI

[10.1029/2020WR027298](https://doi.org/10.1029/2020WR027298)

Publication date

2020

Document Version

Final published version

Published in

Water Resources Research

Citation (APA)

Gao, W., Nienhuis, J., Nardin, W., Wang, Z., Shao, D., Sun, T., & Cui, B. (2020). Wave Controls on Deltaic Shoreline-Channel Morphodynamics: Insights From a Coupled Model. *Water Resources Research*, 56(9), 1-14. Article e2020WR027298. <https://doi.org/10.1029/2020WR027298>

Important note

To cite this publication, please use the final published version (if applicable).

Please check the document version above.

Copyright

Other than for strictly personal use, it is not permitted to download, forward or distribute the text or part of it, without the consent of the author(s) and/or copyright holder(s), unless the work is under an open content license such as Creative Commons.

Takedown policy

Please contact us and provide details if you believe this document breaches copyrights.

We will remove access to the work immediately and investigate your claim.

Water Resources Research

RESEARCH ARTICLE

10.1029/2020WR027298

Special Section:

Coastal hydrology and oceanography

Key Points:

- Waves can deflect deltaic channels, thereby enhancing river mouth progradation and riverbed aggradation and reducing avulsion timescale
- The trade-off effects of waves on deltaic channels depend on wave diffusivity, sediment bypassing, and alongshore sediment transport
- Empirical formulas are proposed to predict the progradation, aggradation, and avulsion of deltaic channels under (a)symmetric wave climates

Supporting Information:

- Supporting Information S1
- Table S1

Correspondence to:

D. Shao,
ddshao@bnu.edu.cn

Citation:

Gao, W., Nienhuis, J., Nardin, W., Wang, Z. B., Shao, D., Sun, T., & Cui, B. (2020). Wave controls on deltaic shoreline-channel morphodynamics: Insights from a coupled model. *Water Resources Research*, 56, e2020WR027298. <https://doi.org/10.1029/2020WR027298>

Received 9 FEB 2020

Accepted 29 JUL 2020

Accepted article online 3 AUG 2020

Wave Controls on Deltaic Shoreline-Channel Morphodynamics: Insights From a Coupled Model

Weilun Gao^{1,2,3}, Jaap Nienhuis⁴ , William Nardin⁵ , Zheng Bing Wang^{1,6,7} , Dongdong Shao^{1,3,8} , Tao Sun^{1,3} , and Baoshan Cui^{1,3}

¹State Key Laboratory of Water Environment Simulation and School of Environment, Beijing Normal University, Beijing, China, ²Research and Development Center for Watershed Environmental Eco-Engineering, Beijing Normal University, Zhuhai, China, ³Yellow River Estuary Wetland Ecosystem Observation and Research Station, Ministry of Education, Shandong, China, ⁴School of Geosciences, Utrecht University, Utrecht, Netherlands, ⁵Horn Point Laboratory, University of Maryland Center for Environmental Science, Cambridge, MD, USA, ⁶Deltires, Delft, Netherlands, ⁷Faculty of Civil Engineering and Geosciences, Delft University of Technology, Delft, Netherlands, ⁸Tang Scholar, Beijing Normal University, Beijing, China

Abstract It is widely recognized that waves inhibit river mouth progradation and reduce the avulsion timescale of deltaic channels. Nevertheless, those effects may not apply to downdrift-deflected channels. In this study, we developed a coupled model to explore the effects of wave climate asymmetry and alongshore sediment bypassing on shoreline-channel morphodynamics. The shoreline position and channel trajectory are simulated using a “shoreline” module which drives the evolution of the river profile in a “channel” module by updating the position of river mouth boundary, whereas the channel module provides the sediment load to river mouth for the “shoreline” module. The numerical results show that regional alongshore sediment transport driven by an asymmetric wave climate can enhance the progradation of deltaic channels if sediment bypassing of the river mouth is limited, which is different from the common assumption that waves inhibit delta progradation. As such, waves can have a trade-off effect on river mouth progradation that can further influence riverbed aggradation and channel avulsion. This trade-off effect of waves is dictated by the net alongshore sediment transport, sediment bypassing at the river mouth, and wave diffusivity. Based on the numerical results, we further propose a dimensionless parameter that includes fluvial and alongshore sediment supply relative to wave diffusivity to predict the progradation and aggradation rates and avulsion timescale of deltaic channels. The improved understanding of progradation, aggradation, and avulsion timescale of deltaic channels has important implications for engineering and predicting deltaic wetland creation, particularly under changing water and sediment input to deltaic systems.

1. Introduction

River deltas host more than half a billion people worldwide and are among the most productive ecosystems on the planet (Giosan et al., 2014; Syvitski et al., 2009). Morphodynamics of deltaic channels such as avulsions play a critical role in the evolution of river deltas and restoration of coastal wetlands and, therefore, have been studied extensively (Chatanantavet et al., 2012; Edmonds et al., 2009; Fisk, 1952; Ganti et al., 2016; Jerolmack & Swenson, 2007; Nienhuis et al., 2018; Smith et al., 1989). Delta progradation can lead to riverbed aggradation with respect to its floodplain, which in turn is thought to increase the likelihood of channel avulsion (Chadwick et al., 2019; Ganti et al., 2014; Mohrig et al., 2000; Zheng et al., 2018). As such, studying the controls on river mouth progradation is critical to better understand channel avulsions (Chadwick et al., 2019).

The progradation of deltaic channel is subject to downstream controls such as basin water depth and waves (Bijkerk et al., 2016; Wang et al., 2019; Zheng et al., 2018). Among these factors, waves tend to reduce the seaward progradation of deltaic channels when low-angle waves (i.e., when the angle between wave crests and the shoreline is smaller than 45°) are dominant, which further suppress the aggradation of deltaic channels and thus increase the avulsion timescale (Ashton & Giosan, 2011; Ratliff et al., 2018; Swenson, 2005). However, previous studies including those mentioned above generally focused on the effects of symmetric

wave climates on the progradation and avulsion timescale of deltaic channels. Under asymmetric wave climate, deltaic channels could be deflected with significant net alongshore sediment transport and limited sediment bypassing at river mouths (Bhattacharya & Giosan, 2003; Nienhuis, Ashton, & Giosan, 2016). In such a case, the blockage of alongshore sediment transport at the river mouth could contribute to river mouth progradation (Nienhuis, Ashton, Nardin, et al., 2016) and has cascading effects on the aggradation and avulsion of deltaic channels. As such, the morphodynamics of deltaic channels, namely, progradation, aggradation, and avulsion, are further subject to wave climate asymmetry and sediment bypassing at the river mouth, in addition to the fluvial factors.

In this study, we investigate how waves and fluvial factors control river mouth progradation and lead to cascading effects on riverbed aggradation and avulsion timescales. Since the net alongshore sediment transport and sediment bypassing at river mouth are determined by the long-term wave climate and fluvial input of water and sediment, we further seek to quantify and predict the abovementioned morphodynamic behaviors of deltaic shoreline-channel system from boundary conditions. Better understanding the relevant effects of waves on the morphodynamics of deltaic shoreline-channel systems helps quantify the avulsion timescale of deltaic channels and predict the future evolution of river deltas under global changes such as reduced fluvial sediment supply. For example, the Yellow River Delta (Wang & Liang, 2000) and the Ebro Delta (Canicio & Ibáñez, 1999), which have gone through multiple historical avulsions, are shifting towards wave-dominated regime due to decreasing fluvial sediment input (Nienhuis et al., 2020), and presumably subject to more significant wave effects on their progradation and avulsion timescales going forward.

To address these issues, we developed a coupled model of shoreline and deltaic channel evolution (section 3) to investigate morphodynamics of deltaic channels under different combinations of river discharge, fluvial sediment input, wave climate, and the other relevant modeling parameters (section 4). We further discuss the trade-off effects of waves on the morphodynamics of deltaic channels (section 5.1) and propose a conceptual model to predict the morphodynamic evolution of deltaic channels, which is tested by the numerical results from this study (section 5.2) and compared with numerical and field data from previous studies (section 5.3).

2. Background

2.1. Wave Influence on the Progradation of Deltaic Channels

As shown in Figures 1a–1h, deltaic channels can prograde perpendicular to the regional shoreline, migrate updrift, or deflect downdrift in the direction of alongshore sediment transport (termed “downdrift-deflected” hereinafter). When a deltaic channel is perpendicular or migrates updrift to the regional shoreline, wave-driven alongshore sediment transport redistributes the fluvial sediment input away from the river mouth (Figures 1j and 1k). As a result, the progradation rate decreases with increasing portion of low-angle waves or wave height due to the increasing wave-induced sediment transport away from the river mouth, that is, the effects of wave diffusivity (Ashton & Giosan, 2011; Swenson, 2005).

However, when deltaic channel is downdrift-deflected, wave-driven alongshore sediment transport can contribute to sediment deposition at the river mouth (Figure 1l) (Ashton & Giosan, 2011; Dominguez, 1996; Nienhuis, Ashton, & Giosan, 2016; Nienhuis, Ashton, Nardin, et al., 2016). Therefore, the progradation of deltaic channels in the presence of waves is subject to (1) the net alongshore sediment transport driven by wave climate asymmetry (Nienhuis, Ashton, & Giosan, 2016) and (2) sediment bypassing at the river mouth which is in turn controlled by the interaction between fluvial water and sediment discharge and wave climate (Nienhuis, Ashton, Nardin, et al., 2016).

2.2. Alongshore sediment bypassing at river mouth

At the river mouth, fluvial discharge and waves interact to block alongshore sediment transport (the “hydraulic groin” effect, Zenkovich (1967)), which primarily depends on the interaction between waves and river discharge (Bakker & Edelman, 1964; Grijm, 1960; Nienhuis, Ashton, Nardin, et al., 2016; Zenkovich, 1967). Nienhuis, Ashton, Nardin, et al. (2016) studied river mouths using Delft3D model experiments and found that river mouths with relatively high ocean wave momentum allow for high alongshore sediment bypassing, whereas river flow jet momentum tends to reduce bypassing. Based on their study,

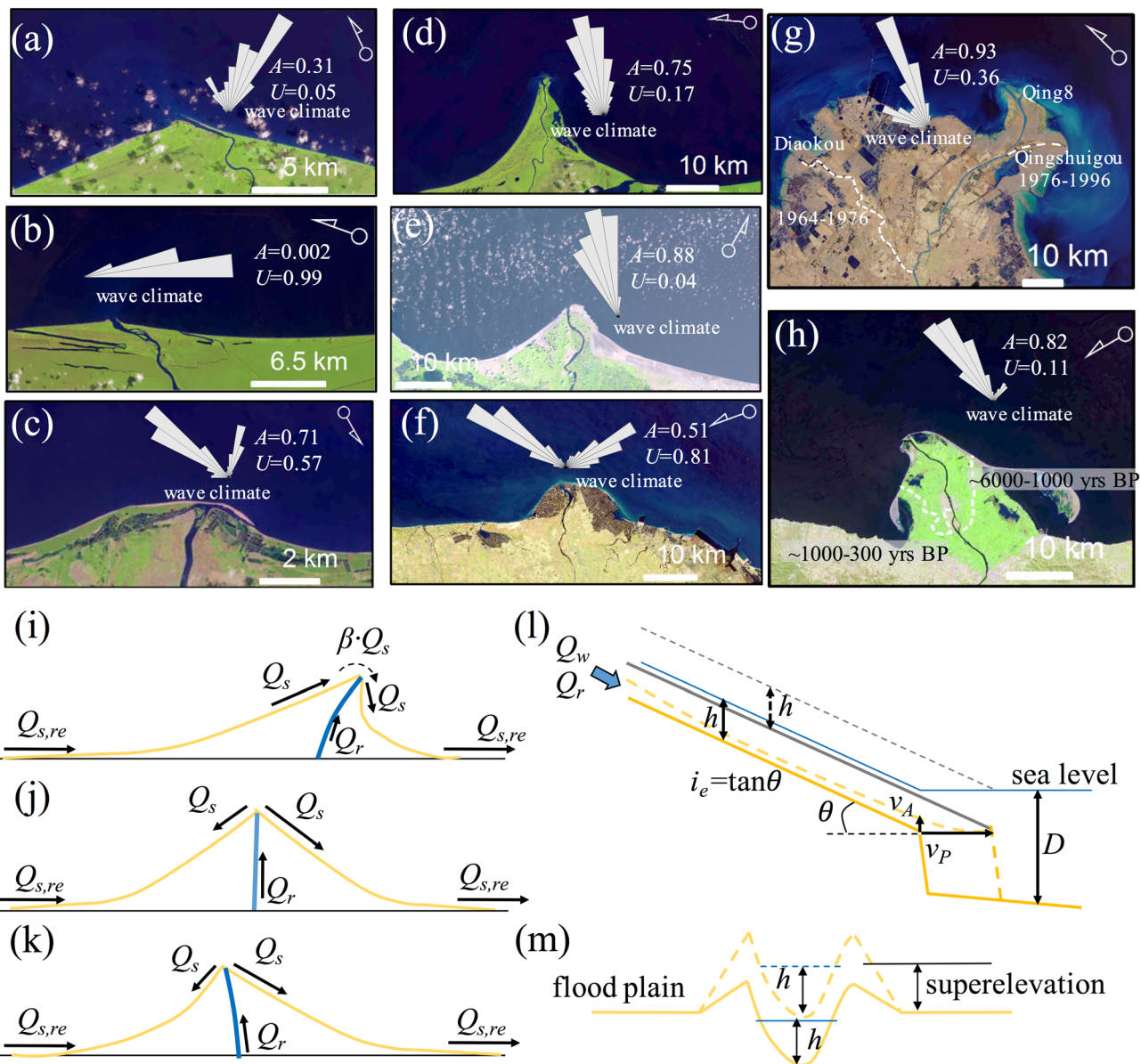


Figure 1. Wave-influenced river deltas with deflected deltaic channels: (a) Patuca River, Honduras, (b) Rio Colorado River, Costa Rica, and (c) Hainan Wanglou River, China; and “perpendicular” deltaic channels: (d) Coco River, Honduras, (e) Rosetta lobe of the Nile River Delta, Egypt, and (f) Luanhe River, China. Also, historical avulsions of deltaic channels (black dashed lines) in (g) Yellow River Delta, China, and (h) Ebro Delta, Spain. Schematics of alongshore sediment transport for (i) downdrift-deflected, (j) perpendicular, and (k) updrift-migrated deltaic channels; and aggrading riverbed under river mouth progradation: (l) longitudinal profile and (m) cross-sectional profile, where the solid yellow line is the initial riverbed, the dashed yellow and solid gray line are the actual and equilibrium riverbeds, respectively, and the solid blue and gray dashed lines are the initial and equilibrium water surface, respectively. Angular distributions of wave energy approaching the shoreline are from WaveWatch III® (Chawla et al., 2013). Remote sensing images are from the EarthExplorer of USGS.

the fraction of alongshore sediment transport bypassing the river mouth β obeys the following empirical relationship:

$$\beta = \frac{1}{1 + 10 \cdot J^3} \quad (1)$$

J is a dimensionless river mouth balance. β tends to 0 for high values of J , it tends to 1 for low values of J . J is defined as

$$J = \frac{M_j}{M_w} \cdot \frac{Q_s}{Q_s + Q_r} \quad (2)$$

where M_j and M_w (kg m/s^2) are the momentum of river flow jet and waves at the river mouth (see Nienhuis, Ashton, Nardin, et al. (2016) for the detailed definitions), respectively, Q_s (m^3/s) is the alongshore sediment transport at the river mouth, and Q_r (m^3/s) is the fluvial sediment input.

Previous studies showed that the orientation of deltaic channels can be predicted from wave forcing such as net alongshore sediment transport and fluvial forcing such as river discharge and sediment load, as well as alongshore sediment bypassing at river mouth (Bhattacharya & Giosan, 2003; Nienhuis, Ashton, & Giosan, 2016). In this study, we further investigate the progradation of deltaic channels and its cascading effects on riverbed aggradation and avulsion timescale under symmetric and asymmetric wave climates and limited alongshore sediment bypassing at river mouth.

2.3. Riverbed Aggradation and Avulsion of Deltaic Channels Under River Mouth Progradation

As shown in Figure 1l, the progradation of the deltaic channel, in principle, decreases the river relief, causing in-channel sedimentation and the aggradation of the riverbed (Muto & Swenson, 2005). Riverbed aggradation relative to its floodplain can set up conditions favorable for channel avulsions (Figure 1m). Such conditions can be quantified by a threshold lateral slope advantage or superelevation of the channel bed relative to its floodplain (Mohrig et al., 2000; Zheng et al., 2018). The superelevation hypothesis, which states that avulsion occurs when the superelevation of the channel belt reaches a specified fraction α of the channel depth, h (Chadwick et al., 2019; Ganti et al., 2014; Mohrig et al., 2000; Moodie et al., 2019), was adopted in this study for avulsion setup.

Potential wave effects on suppressing riverbed aggradation and increasing avulsion timescale are based on the assumption that waves tend to reduce river mouth progradation. Previous studies have showed that the evacuation of sediment from the river mouth due to waves reduces the seaward progradation and aggradation rates of deltaic channels and thus increases the avulsion timescale (Swenson, 2005). Ratliff et al. (2018) further reported that increasing wave height results in longer avulsion timescale when low-angle waves are dominant, presumably due to their tendency to transport sediment away from the river mouth. However, waves can enhance the progradation of downdrift-deflected deltaic channels when alongshore sediment transport contributes to sediment deposition at the river mouth, but the relevant effects on the aggradation and avulsion timescale of deltaic channels are still unclear.

3. Model Development

3.1. Governing Equations

We developed a coupled morphodynamic model for the integrated evolution of deltaic channels and shorelines (Figures 2a and 2b), which consists of two modules: (1) the “shoreline” module that simulates the evolution of the shoreline under waves and (2) the “channel” module that simulates the evolution of the longitudinal profile of the deltaic channel. We used the Coastline Evolution Model (CEM) to simulate deltaic shoreline evolution. CEM is a one-line shoreline model that simulates shoreline evolution based on gradients in alongshore sediment transport (Ashton and Murray (2006)). Nienhuis, Ashton, and Giosan (2016) later expanded CEM to study wave-influenced deltas by including channels that prograde perpendicularly to the local shoreline orientation at the river mouth. Here, we adopted the updated CEM model to simulate the progradation of deltaic channels. Model details can be found in Ashton and Murray (2006) and Nienhuis, Ashton, and Giosan (2016). Briefly, the governing equations for volumetric alongshore sediment transport and shoreline evolution read

$$Q_s = K_1 H_b^{5/2} \cos(\phi_b - \phi) \sin(\phi_b - \phi) \quad (3)$$

$$\frac{dy_s}{dt} = -\frac{1}{D} \frac{dQ_s}{dx_s} \quad (4)$$

where K_1 ($\text{m}^{0.5}/\text{s}$) is an empirical coefficient for alongshore sediment transport, H_b (m) is the average breaking wave height, ϕ_b and ϕ are wave approaching and shoreline angles, respectively, D (m) is the

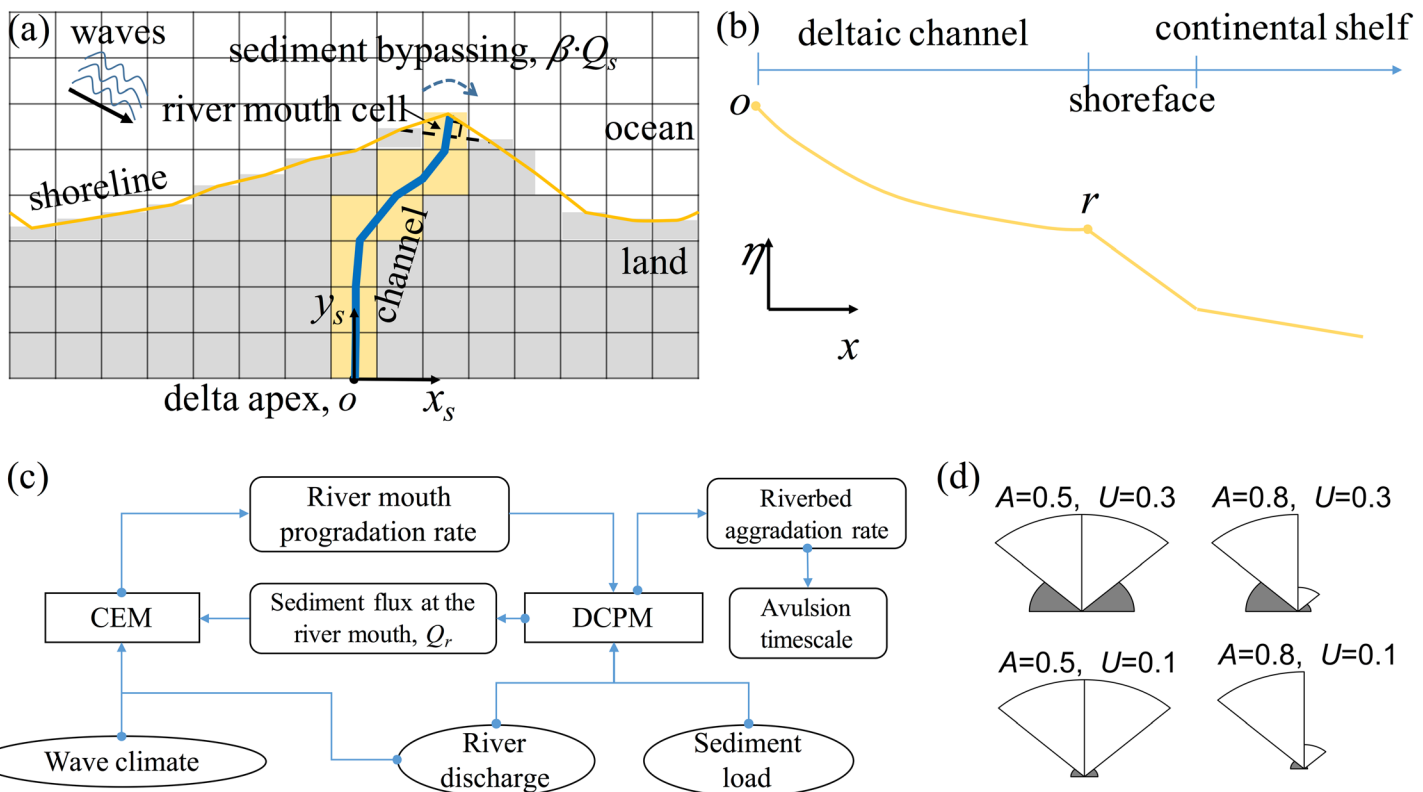


Figure 2. Schematic of the evolution of the shoreline and deltaic channel: (a) plain view and (b) cross-section along the deltaic channel, shoreface, and continental shelf. x_s and y_s are the alongshore and cross-shore coordinates, respectively, with the origin of the coordinates located at the delta apex O . η and x are bed level and downstream distance along the deltaic channel. (c) Coupling between the Coastline Evolution Model and Deltaic Channel Profile Model. Elliptical boxes present boundary conditions, rectangular boxes present modules, and rounded rectangular boxes present simulation results. (d) Schematics of wave climates using wave climate asymmetry, A , and fraction of high-angle waves (shaded portion), U , following Ashton and Murray (2006).

nearshore water depth, x_s and y_s are alongshore and cross-shore distance, respectively, and t (s) is time. Equation 3 in the case of deep-water waves becomes

$$Q_s = K_2 H_0^{12} T_0^{\frac{1}{5}} \cos^{\frac{6}{5}}(\phi_0 - \phi) \sin(\phi_0 - \phi) \quad (5)$$

K_2 ($m^{0.6}/s^{1.2}$) is an empirical coefficient for deep-water alongshore sediment transport, H_0 (m), T_0 (s), and ϕ_0 are the average deep-water wave height, period, and approaching angle, respectively. Substituting Equation 5 into Equation 4 and using the chain rule yield

$$\frac{dy_s}{dt} = -\kappa \frac{d^2 y_s}{dx_s} \quad (6)$$

where wave diffusivity κ (m^2/s) is wave angle dependent:

$$\kappa = \frac{K_2}{D} H_0^{\frac{12}{5}} T_0^{\frac{1}{5}} \left\{ \cos^{\frac{1}{5}}(\phi_0 - \phi) \left[\cos^2(\phi_0 - \phi) - \frac{6}{5} \sin^2(\phi_0 - \phi) \right] \right\} \quad (7)$$

We discretized the shoreline model into cells (Figure 2a), where one cell is defined as the river mouth cell which is fed by fluvial sediment from the deltaic channel.

We simulated fluvial sediment supply at the river mouth as well as the riverbed aggradation using the channel module, that is, the Deltaic Channel Profile Model (DCPM). We developed the module by solving the set of 1-D steady Saint-Venant equations (Chow, 1959), a general power law for sediment transport capacity (Jansen et al., 1979) and the Exner equation (Paola & Voller, 2005), which are

$$h \frac{\partial u}{\partial x} + u \frac{\partial h}{\partial x} = 0 \quad (8)$$

$$u \frac{\partial u}{\partial x} + g \frac{\partial h}{\partial x} + g \frac{\partial \eta}{\partial x} + C_f \frac{u^2}{h} = 0 \quad (9)$$

$$Q_r = Bmu^n \quad (10)$$

$$(1 - \lambda) \frac{\partial \eta}{\partial t} = - \frac{1}{B} \frac{\partial Q_r}{\partial x} \quad (11)$$

where h (m) is water depth, x (m) is the downstream distance of the river channel, $u = Q_w/Bh$ (m/s) is the flow velocity in which Q_w (m^3/s) is the river discharge, η (m) is bed level, g (m/s^2) is gravitational acceleration, $C_f = g/C_z^2$ is the dimensionless friction coefficient in which C_z ($\text{m}^{0.5}/\text{s}$) is the Chezy coefficient, Q_r (m^3/s) is the sediment transport, B (m) is the channel width, m and n are coefficients in empirical sediment transport formula, and λ is porosity. Notably, we used the Engelund-Hansen formula for total bed-material transport (Engelund & Hansen, 1967) with $m = \frac{0.05C_f^{1.5}}{(Rsg)^2 D_{50}}$ and $n = 5$, where R_s (=1.65) is submerged specific density of sediment. Other sediment transport formulas such as the Einstein-Brown formula (Brown, 1950) and the Generalized Engelund-Hansen sediment transport formula (Ma et al., 2017; Ma et al., 2020) can also be applied by changing the empirical coefficients of m and n in Equation 10.

The coupling between CEM and DCPM is shown in Figure 2c. At every model iteration, we firstly calculated the fluvial sediment input at the river mouth Q_r by DCPM, which was further used as the sediment supply to the shoreline in CEM. Afterwards, we calculated alongshore sediment bypassing at the river mouth in CEM through Nienhuis, Ashton, Nardin, et al. (2016)'s formula, that is, Equation 1. Then we simulated the shoreline evolution, the position of the river mouth $r(t)$ and the trajectory of the deltaic channel in CEM, which dictates the length of the deltaic channel and updates the downstream position of the river mouth in DCPM. Notably, we did not explicitly simulate avulsions in the coupled model, but adopted the superelevation hypothesis for avulsion setup and assumed $\alpha = 1$ (Ratliff et al., 2018; Swenson, 2005). Furthermore, we assumed the avulsion location is at an upstream distance of L_b (backwater length) from the river mouth at the end of the simulation period. As such, we determined avulsion timescale by dividing the channel depth by the aggradation rate at an upstream distance of L_b from the river mouth (Figure 2c). This is in contrast to the study of Ratliff et al. (2018) who simulated multiple avulsion cycles. Notably, the backwater length is estimated as $L_b = h_e/i_e$ (Paola & Mohrig, 1996), where h_e and i_e are the equilibrium water depth and slope of the river channel in this study which can be derived from Equations 9 and 10 following Wang et al. (2008).

3.2. Boundary Conditions

For CEM, we used periodic boundary conditions at the left and right cross-shore boundaries for alongshore sediment flux, which assumes that deltas evolve along an infinitely long coastline with a continuous alongshore sediment supply from the updrift coast, that is,

$$Q_s(x_s = x_{s,l}, t) = Q_s(x_s = x_{s,r}, t) \quad (12)$$

where $x_{s,l}$ and $x_{s,r}$ are the shoreline position at the left and right cross-shore boundaries, respectively. The simulation domain for CEM is large enough relative to the simulated deltas such that the delta is devoid of the influences of the boundaries. For DCPM, we imposed a constant bankfull discharge, Q_{w0} and sediment load, Q_{r0} , at the upstream boundary of the river channel and a constant water level H (m) at the downstream boundary, which read

$$Q_w(x = 0, t) = Q_{w0} \quad (13)$$

$$Q_r(x = 0, t) = Q_{r0} \quad (14)$$

$$H(x = x_r, t) = 0 \quad (15)$$

where x_r (m) is the downstream position of the river mouth.

3.3. Modeling Parameters

We start the model simulations with a straight shoreline perpendicular to the initial river channel. The shoreface and shelf slope are 0.01 and 0.001, respectively, and the shoreface depth are 10 and 15 m between different simulations. The width of the river channel is 100 m, and the initial riverbed has a quasi-linear profile with an equilibrium slope i_e and an equilibrium water depth h_e . The initial river length ranges from 200 to 500 km, which is larger than two times the backwater length L_b . The cell width (100 m) in CEM is identical to the channel width in DCPM. The simulation period was set as 100 years for all simulation scenarios, which is sufficient for the modeled deltaic channels to reach stable gradual evolution resembling natural channels. The time step for the CEM is 1 day, and the time step for the DCPM is 0.01 day.

As shown in Figure 2d, we use two parameters to characterize wave climates following Ashton and Murray (2006): the fraction of waves coming from the left looking offshore (wave climate asymmetry, A) and the fraction of waves coming from high angles (approaching angle $>45^\circ$, U). We vary wave climate asymmetry from 0.5 to 0.8, and the portion of high-angle waves from 0.1 and 0.3 between different simulations, corresponding to diffusive waves climates. Offshore wave height H_0 is varied between 0.8 and 2.5 m, and the wave period T_0 is fixed at 5 s. Deep-water alongshore sediment transport coefficient K_2 ranges from 0.015 to 0.15 $\text{m}^{0.6}/\text{s}^{1.2}$ between different simulations.

The river discharge Q_w and sediment concentration C_s range from 50 to 800 m^3/s and 0.1 to 0.5 kg/m^3 between experiments, respectively, which together result in fluvial sediment input (i.e., bed-material load) of 10–80 kg/s . The combinations of river discharge and sediment load were derived to span small to medium rivers (Caldwell et al., 2019), such as the Ebro (Nienhuis et al., 2017) and the Brazos (Rodriguez et al., 2000). We model noncohesive sediments with a uniform grain size (D_{50}) which are 65 and 150 μm . Bed porosity λ is 0.4, and sediment density is 2,650 kg/m^3 . We use dimensionless friction coefficients C_f of 0.0011 and 0.0039. The combinations of modeling parameters for different scenarios are documented in Table S1 in the supporting information.

We use two dimensionless parameters to characterize the model results: (1) the river dominance ratio R (Nienhuis et al., 2015) which compares fluvial sediment input Q_r relative to the maximum possible alongshore sediment transport away from river mouth $Q_{s,max}$ and (2) sediment source ratio S (Nienhuis, Ashton, & Giosan, 2016) which compares the regional net alongshore sediment transport driven by the wave climate asymmetry $Q_{s,re}$ to fluvial sediment input Q_r , that is,

$$R = \frac{Q_r}{Q_{s,max}} \quad (16)$$

and

$$S = \frac{Q_{s,re}}{Q_r} \quad (17)$$

River deltas have a wave-dominated morphology if $R < 1$ and a river-dominated morphology for $R > 1$ (Nienhuis et al., 2015). Downdrift deflection of deltaic channels on the other hand scales with $S \cdot (1 - \beta)$ (Nienhuis, Ashton, & Giosan, 2016). We calculate $Q_{s,max}$ and $Q_{s,re}$ following Nienhuis et al. (2015) and Nienhuis, Ashton, and Giosan (2016), respectively. The various combinations of modeling parameters result in river dominance ratios R ranging from 0.01 to 13.5 and sediment source ratios S ranging from 0 to 27, representing deltas varying from river-dominated to wave-dominated ones.

4. Results

As shown in Figure 3, river deltas attain a symmetric plan form when wave climate is symmetric ($A = 0.5$, the first column panels of Figure 3) and migrate updrift when fluvial sediment input is dominant and wave approach at an angle (R is relatively high and $S > 0$, the second to fourth panels in the first row of Figure 3). However, as shown in the right panels of Figure 3, deltaic channels become downdrift-deflected with decreasing R and increasing wave climate asymmetry (and hence increasing S). Those results are consistent with the original model simulations from Nienhuis, Ashton, and Giosan (2016).

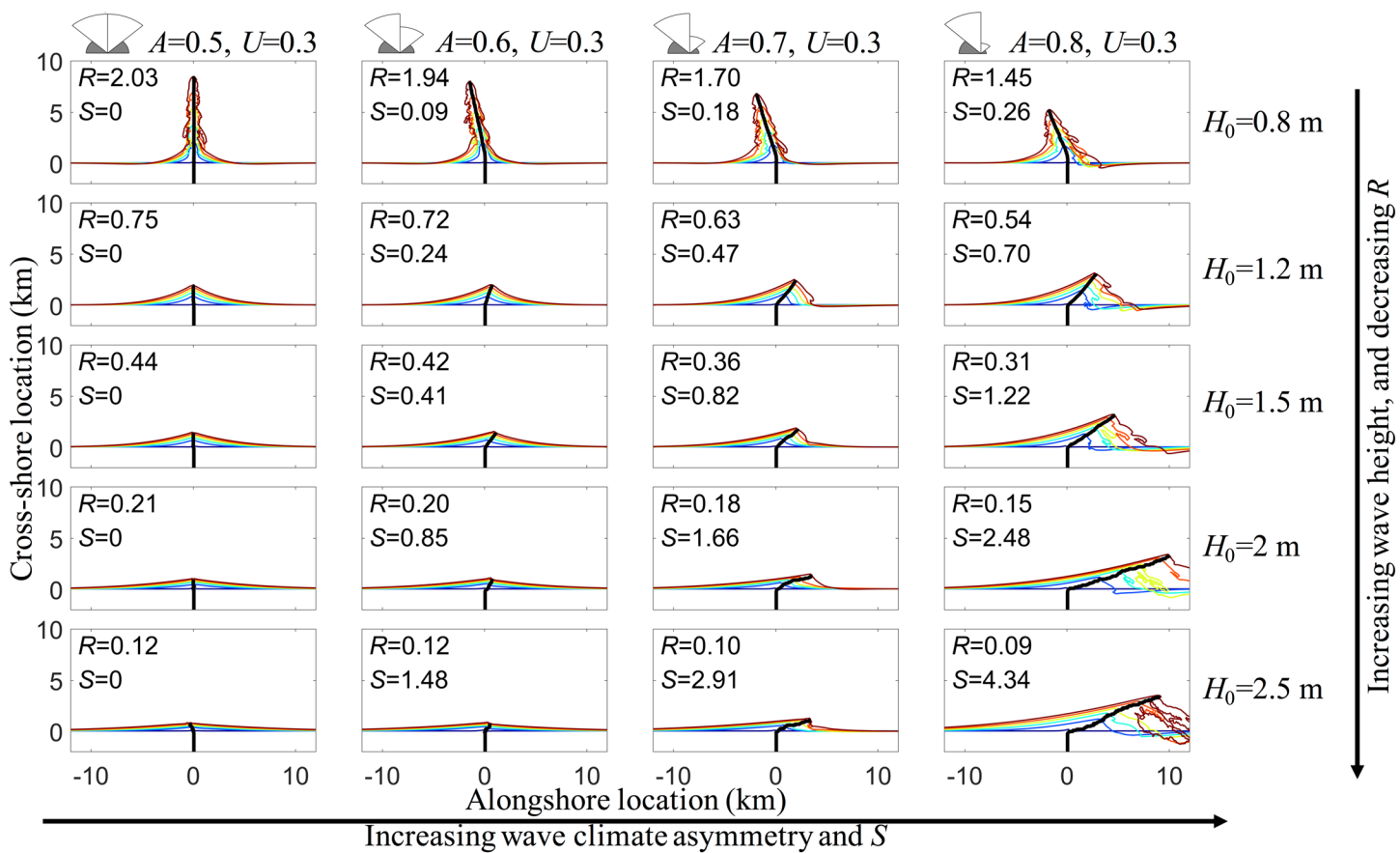


Figure 3. Evolution of river deltas for representative numerical experiments with different wave climates for which $Q_w = 600 \text{ m}^3/\text{s}$, $Q_r = 60 \text{ kg/s}$, $D = 10 \text{ m}$, $D_{50} = 65 \mu\text{m}$, and $K_2 = 0.15 \text{ m}^{0.6}/\text{s}^{1.2}$. The black lines represent the planar trajectory of deltaic channel at the end of the simulation period (100 years), and the colored lines indicate the simulated shoreline position every 20 years.

When the wave climate is symmetric or fluvial sediment input is dominant such that river deltas attain a symmetric plan form or migrate updrift, the wave-driven alongshore sediment transport redistributes the fluvial sediment input away from the river mouth, that is, the effects of wave diffusivity (Ashton & Giosan, 2011; Nienhuis, Ashton, & Giosan, 2016; Swenson, 2005). In this case, increasing wave height and hence wave diffusivity reduces the progradation of deltaic channels (Figure 4a). Suppression of river mouth progradation could reduce the riverbed aggradation rate and increase the avulsion timescale (Figures 4b and 4c), which is consistent with previous studies (Swenson, 2005).

However, when the net regional alongshore sediment transport is large and sediment bypassing is limited such that a deltaic channel is downdrift-deflected, increasing wave climate asymmetry and wave height result in increasing net alongshore sediment transport (Equation 3), which could enhance the progradation of deltaic channels with limited sediment bypassing at the river mouth, despite the increasing wave diffusivity (Figures 4a and 4d). In this case, the enhanced river mouth progradation under waves could lead to increased riverbed aggradation rate and decreased avulsion timescale (Figures 4b, 4c, and 4e), an exactly opposite trend from above. Notably, the aggradation rate was calculated at an upstream distance of L_b (back-water length) from the river mouth, and avulsion setup is attained when aggradation of the riverbed equals to the channel depth.

5. Discussion

5.1. Trade-off Effects of Waves on Morphodynamics of Deltaic Channels

We observed that an increasing wave height under asymmetric wave climates poses two counteracting effects on the progradation of deltaic channels (Figure 5):

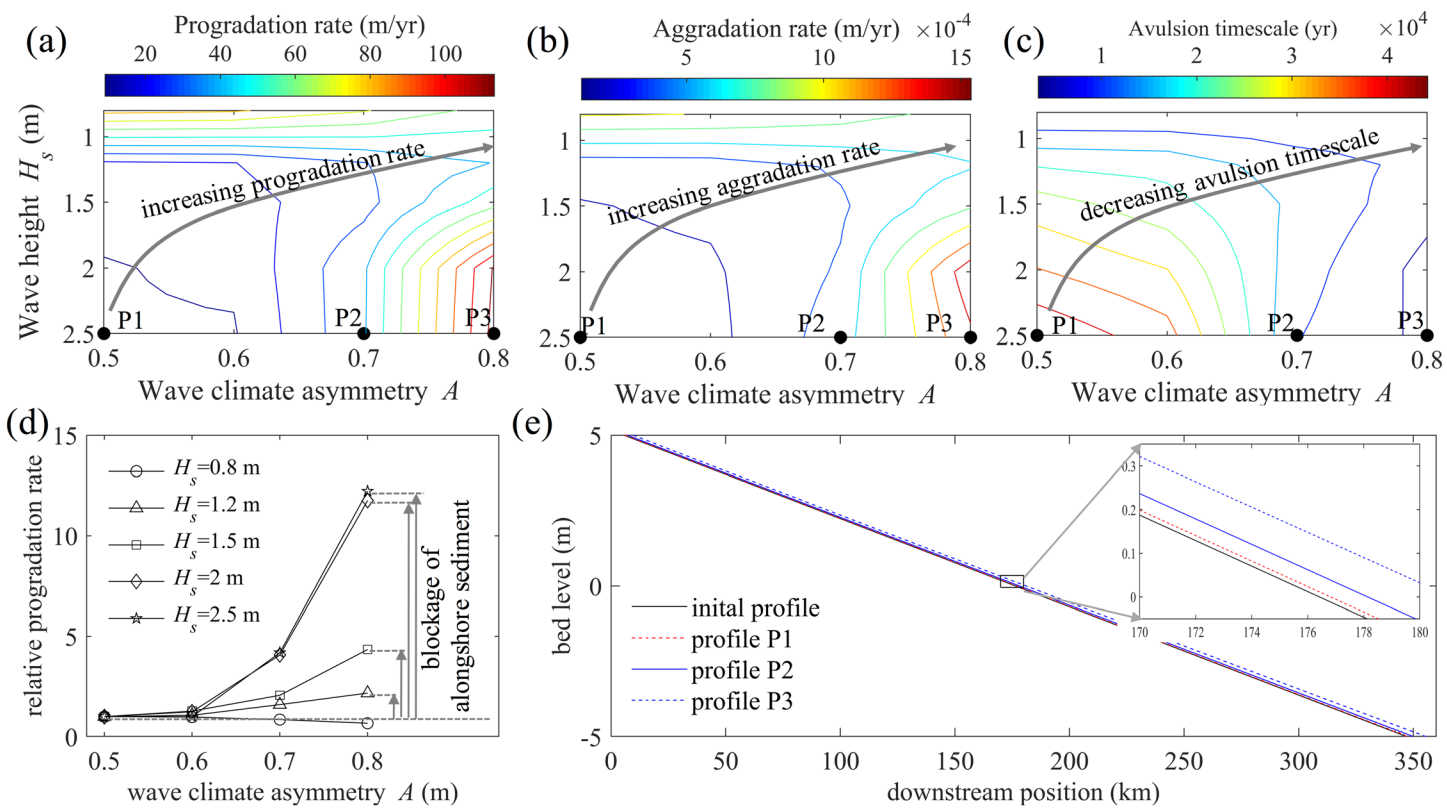


Figure 4. Contour plots of (a) progradation rate, (b) aggradation rate, and (c) calculated avulsion timescale in the parameter space of wave height and wave climate asymmetry for scenarios shown in Figure 3. (d) Relative progradation rate against wave climate asymmetry, after normalized by corresponding scenarios under symmetric wave climate scenarios. (e) Representative river longitudinal profiles indicated in panels a–c.

1. increasing net alongshore sediment transport $Q_{s,re}$ (Figure 5a) and hence the progradation of downdrift-deflected deltaic channels with limited sediment bypassing (Figure 5d), which further leads to increasing aggradation rate and decreasing avulsion timescale of deltaic channels (Figures 5e and 5f); and concurrently
2. increasing sediment bypassing β (Equation 1) and wave diffusivity κ (Equation 7), which could offset the abovementioned effects of increasing net alongshore sediment transport (Figures 5b and 5c) and further result in decreasing aggradation rate and increasing avulsion timescale of deltaic channels (Figure 5e and 5f).

Therefore, the net effects of waves presumably depend on the trade-off between the wave-induced increasing net alongshore sediment transport, sediment bypassing and wave diffusivity, that is, the river mouth progradation tends to be positively proportional to net alongshore sediment transport $Q_{s,re}$ and negatively proportional to sediment bypassing β and wave diffusivity κ , which leads to the inflection point in the curve of river mouth progradation rate, as well as those of the aggradation rate of the riverbed and avulsion timescale.

5.2. Predicting the Progradation, Aggradation, and Avulsion Timescale of Deltaic Channels

To quantify the trade-off effects of waves on the progradation of deltaic channels, a conceptual model following Nienhuis, Ashton, Nardin, et al. (2016) and Swenson (2005) is illustrated as follows. For downdrift-deflected deltas (Figure 1i), river mouth progradation scales with the fluvial sediment supply as well as the potential captured alongshore sediment by the river mouth,

$$Q_{total} = Q_r + Q_{s,re} \cdot (1 - \beta) \quad (18)$$

Notably, when deltas attain a symmetric plan form or migrate updrift, the wave-driven alongshore sediment transport is away from the river mouth (Figures 1j and 1k). As such, the net alongshore sediment transport does not contribute to the sediment deposition at the river mouth, that is, $Q_{total} = Q_r$. In our

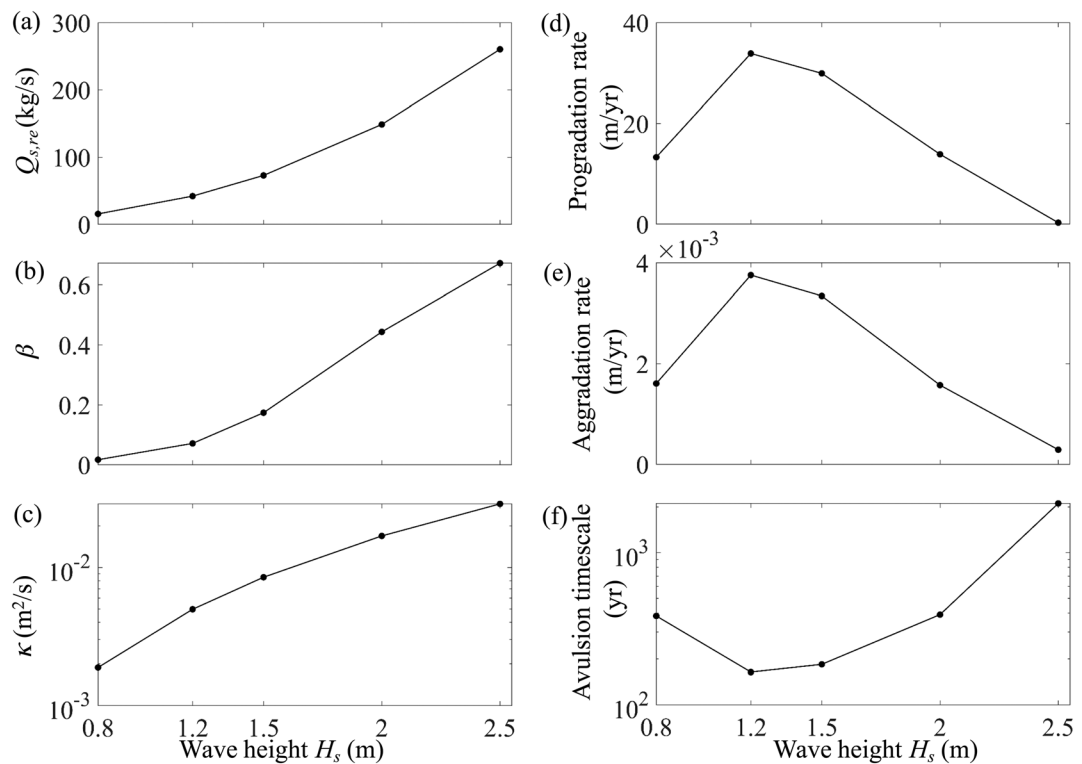


Figure 5. (a) Net regional alongshore sediment transport $Q_{s,re}$, (b) sediment bypassing β , (c) wave diffusivity κ , (d) progradation rate, (e) aggradation rate, and (f) avulsion timescale of deltaic channels against wave heights for numerical experiments with downdrift-deflected deltaic channels ($Q_w = 50 \text{ m}^3/\text{s}$, $Q_s = 10 \text{ kg/s}$, $A = 0.8$, $U = 0.3$, $D = 15 \text{ m}$, $D_{50} = 65 \mu\text{m}$, and $K_2 = 0.15 \text{ m}^{0.6}/\text{s}^{1.2}$).

numerical simulations, the orientation of the river mouth fluctuates constantly because the wave angles is a distribution characterized by A and U (Figure 2d) and we consider it downdrift-deflected when the average orientation of river mouth is larger than 10 degree downdrift.

Aside from Q_{total} , other significant controls on the progradation rate of deltaic channels v_P (m/s) are the shoreface depth D (m) and wave diffusivity κ (m^2/s). We use these four variables to form two dimensionless variables following Buckingham π theorem (Buckingham, 1914; Sonin, 2004): dimensionless progradation rate $v_{P*} = (v_P \cdot D)/\kappa$ and dimensionless total sediment supply $Q_{total*} = (Q_{total}/D)/\kappa$. In the expression of v_{P*} , $v_P \cdot D$ (m^2/s) can be interpreted as the rate of the infilling of the marine accommodation space per unit width at the river mouth. As for Q_{total*} , Q_{total}/D (m^2/s) represents the ability of sediment supply to infill the marine accommodation space per unit width at the river mouth, whereas κ (m^2/s) is incorporated as a proxy for the acceleration of sediment lost from the river mouth per unit width to alongshore redistribution. Furthermore, calculated using the regional shoreline angle, $Q_{s,re}(1 - \beta)$ and κ are approximation of the alongshore sediment supply and loss, respectively, at the river mouth.

Generally, the increase of Q_{total*} means that more sediment supply tends to deposit at the river mouth against the diffusivity of waves. Limited fluvial sediment input and high sediment bypassing and wave diffusivity (usually associated with relatively strong waves) can result in a low Q_{total*} , whereas considerable fluvial sediment input, relatively weak waves (i.e., κ and β are relatively small) and shallow nearshore waters can lead to a high Q_{total*} .

We further used the numerical results to determine the empirical relationship between v_{P*} and Q_{total*} . We calculated v_P by dividing the total progradation length of the deltaic channel by the simulation period and calculated Q_{total} using Equation 18. The sediment bypassing rate β in Equation 18 is the average sediment bypassing rate of the modeling results. Shoreface depth D is from the model setting and κ follows Equation 7. As shown in Figure 6a, the numerical results of v_{P*} and Q_{total*} collapse fairly well onto a linear relationship in the log-log space ($R^2 = 0.88$), that is,

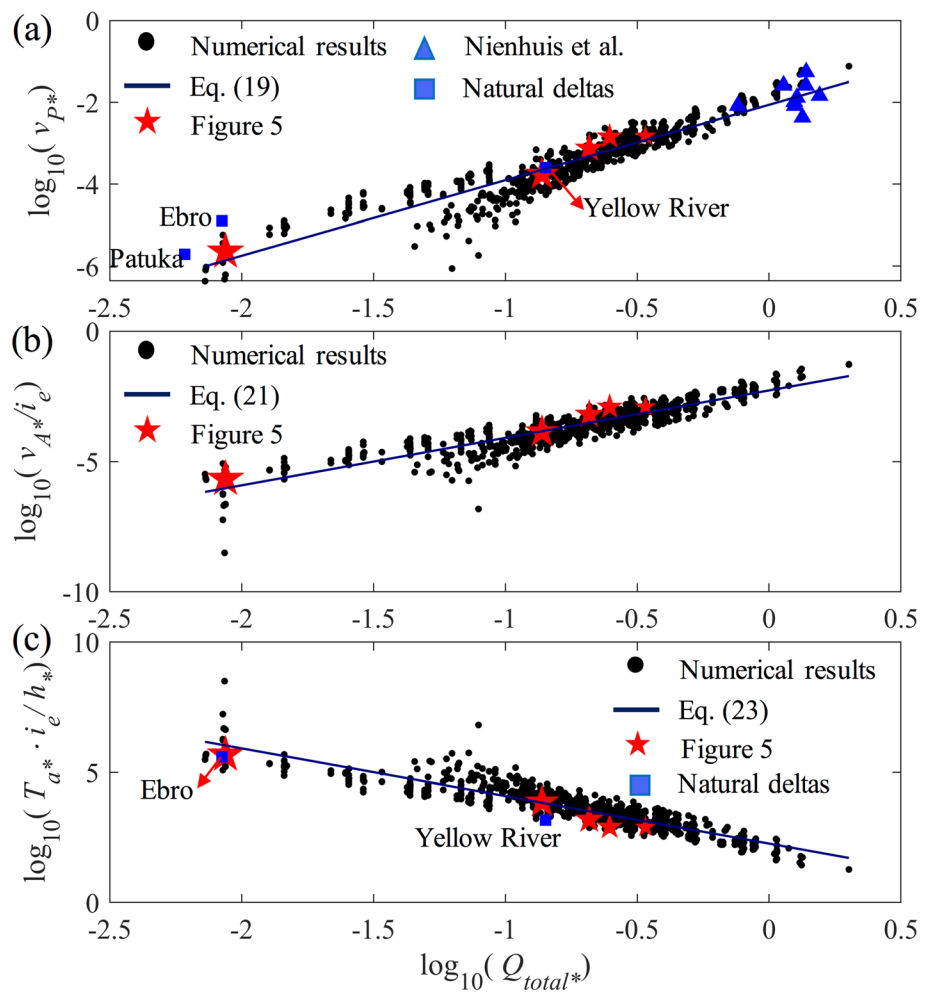


Figure 6. (a) v_{P^*} , (b) v_{A^*}/i_e , and (c) $T_{a^*} \cdot i_e/h_*$ against Q_{total^*} for numerical experiments conducted in this study and from Nienhuis, Ashton, Nardin, et al. (2016) and natural deltas, where v_{P^*} , v_{A^*} , and T_{a^*} are the dimensionless progradation rate, aggradation rate, and avulsion timescale, respectively; Q_{total^*} is the dimensionless total sediment supply to the river mouth; and i_e and h_* are the equilibrium slope and dimensionless water depth of the deltaic channel.

$$v_{P^*} = 0.0088 \cdot Q_{total^*}^{1.8463} \quad (19)$$

To determine the cascading effects of river mouth progradation on riverbed aggradation, we further defined the dimensionless aggradation rate $v_{A^*} = (v_A \cdot D)/\kappa$. Assuming a quasi-linear longitudinal profile with equilibrium slope (Figure 11), we can write the dimensionless aggradation rate of the riverbed v_{A^*} as,

$$v_{A^*} \approx v_{P^*} \cdot i_e \quad (20)$$

where i_e is the equilibrium bed slope following Ganti et al. (2014). We further used the numerical results to determine the relationship between v_{A^*} and Q_{total^*} as follows:

$$v_{A^*}/i_e = 0.0054 \cdot Q_{total^*}^{1.8249} \quad (21)$$

where v_{A^*} is calculated at an upstream distance of L_b (backwater length) from the river mouth. Notably, both the fitted exponent and constant in Equation 21 are smaller than those in Equation 19, which is consistent with the formation of a concave river profile under river mouth progradation (Muto & Swenson, 2005), that is, the progradation of river mouth is faster than the aggradation of the river bed ($v_{A^*}/i_e < v_{P^*}$).

We adopted the superelevation hypothesis for avulsion setup in this study (Figure 1m) and assumed $\alpha = 1$ (Ratliff et al., 2018; Swenson, 2005), and thus, avulsion timescale T_a reads

$$T_a = h_e/v_A \quad (22)$$

where h_e (m) is the equilibrium water depth of the deltaic channel. Substituting Equation 22 into Equation 21 and manipulation lead to

$$T_{a^*} \cdot i_e/h^* = 1/0.0054 \cdot Q_{total^*}^{-1.8249} \quad (23)$$

where $T_{a^*} = T_a/(D^2/\kappa)$ is the dimensionless avulsion timescale and $h^* = h_e/D$ is the dimensionless equilibrium water depth of the deltaic channel which compares the equilibrium channel depth to the shoreface depth. As shown in Figures 6b and 6c, v_{A^*}/i_e and $T_{a^*} \cdot i_e/h^*$ scale well with the dimensionless total sediment supply Q_{total^*} in the log-log spaces ($R^2 = 0.83$). Notably, the avulsion timescale T_a tends to be underestimated as we neglect the floodplain sedimentation (Swenson, 2005). Furthermore, the alongshore migration of river mouth due to the branching of sand spit is not considered an avulsion (Cooper, 1990; Nienhuis, Ashton, Nardin, et al., 2016).

The trade-off effects of increasing wave height on the progradation rate, aggradation rate, and avulsion time-scale of deltaic channels shown in Figure 5 can be further explained by the proposed dimensionless parameterization, that is, v_{P^*} , v_{A^*}/i_e , $T_{a^*} \cdot i_e/h^*$, and Q_{total^*} . As shown in Figure 6, increasing wave height (from 0.8 to 2.5 m, which scales with the size of the red stars) results in a monotonic decrease in Q_{total^*} (from 0.0087 to 0.3398) for scenarios shown in Figure 5, which further results in a steady decrease in v_{P^*} and v_{A^*}/i_e and increase in $T_{a^*} \cdot i_e/h^*$. The results suggest that the dimensionless total sediment supply Q_{total^*} is a potential metric for quantifying the effects of interacting river discharge and wave climate on the morphodynamics of deltaic channels, which unifies the effects of wave angles, wave height, sediment bypassing, shoreface depth, and fluvial sediment input for both symmetric and asymmetric wave climates.

5.3. Comparison With Previous Studies and Natural Deltas

The results of the dimensionless progradation rate of deltaic channels v_{P^*} are compared with the Delft3D simulation results from Nienhuis, Ashton, Nardin, et al. (2016) in Figure 6a. We calculated v_{P^*} and Q_{total^*} using the fluvial sediment input, alongshore sediment transport, wave angle, wave height, wave period, bypassing rate, spite depth, and migration rate from Nienhuis, Ashton, Nardin, et al. (2016). The empirical coefficient for deep-water alongshore sediment transport is estimated as $0.03\text{--}0.05 \text{ m}^{0.6}/\text{s}^{1.2}$ for their simulations. The calculated dimensionless progradation rate and sediment supply from Nienhuis, Ashton, Nardin, et al. (2016) follow the trend of our predictions (Figure 6a). Notably, we used the migration rate from Nienhuis, Ashton, Nardin, et al. (2016) as a proxy of progradation rate for their simulation scenarios with significantly deflected deltaic channels, which generally underestimated the progradation rate.

Relevant field data from representative natural deltas (Guillén & Palanques, 1997; Nienhuis, Ashton, Nardin, et al., 2016; Nienhuis et al., 2017; Zheng et al., 2017) with updrift-migrated (Ebro Delta, Figure 1h), symmetric (Diaokou lobe of the Yellow River Delta, Figure 1g), and downdrift-deflected (Patuka Delta, Figure 1a) deltaic shorelines are shown as blue rectangles in Figure 6. Overall, the dimensionless progradation rate and avulsion timescale against dimensionless total sediment supply to the river mouth from those deltas follow the generic formula derived in our study (see Table S1 in the supporting information). The high fluvial sediment load results in a high Q_{total^*} for the Diaokou Lobe of the Yellow River Delta relative to those for the Ebro Delta and Patuka Delta. As a result, the Yellow River Delta attains a higher progradation rate and shorter avulsion timescale than those of the Ebro Delta and Patuka Delta, which are revealed by the higher v_{P^*} (Figure 6a) and lower $T_{a^*} \cdot i_e/h^*$ (Figure 6c) for the Yellow River Delta.

6. Conclusions

We developed a coupled model of shoreline and river longitudinal profile in this study to explore the interactions between waves and fluvial forcings on the morphodynamics of deltaic channels. The numerical results confirm that the alongshore sediment transport driven by asymmetric wave climate could enhance the progradation of deltaic channels with limited sediment bypassing at the river mouth, which further

increase the aggradation rate and decrease the avulsion timescale. Increasing wave height shows a trade-off effect on the progradation, aggradation, and avulsion timescale of deltaic channels, which depends on the wave-induced relative increase of alongshore sediment transport, sediment bypassing, and wave diffusivity. Dimensional analysis and numerical results suggest a power law relationship between the dimensionless progradation rate, v_{P*} , aggradation rate, v_{A*} , avulsion timescale, T_{a*} , and dimensionless total sediment supply to the river mouth Q_{total*} as a powerful predictive metric for the relevant morphodynamic behavior of deltaic channels.

Data Availability Statement

The data are available at the following website: <https://zenodo.org/record/3660223#.XkAajXsza5s>.

Acknowledgments

This work was supported by the Joint Funds of the National Natural Science Foundation of China (Grant U1806217), the Key Project of National Natural Science Foundation of China (Grant 51639001), and the Interdisciplinary Research Funds of Beijing Normal University. Financial support for Z. B. Wang from the State Administration of Foreign Experts Affairs of China (Grant G20190001540) is also grateful acknowledged. JHN acknowledges support from NWO Grant vi.veni.192.123 and National Science Foundation (NSF) award GLD-1810855. We thank Brad Murray, Andrew Moodie and two anonymous reviewers for their suggestions that helped improve this manuscript.

References

- Ashton, A. D., & Giosan, L. (2011). Wave-angle control of delta evolution. *Geophysical Research Letters*, 38, n/a. <https://doi.org/10.1029/2011GL047630>
- Ashton, A. D., & Murray, A. B. (2006). High-angle wave instability and emergent shoreline shapes: 1. Modeling of sand waves, flying spits, and capes. *Journal of Geophysical Research*, 111, F04011. <https://doi.org/10.1029/2005jf000422>
- Bakker, W. T. J. N. P., & Edelman, T. (1964). The coastline of river-deltas. In B. Edge (Ed.), *Coastal Engineering 1964* (pp. 199–218). Reston, VA: ASCE.
- Bhattacharya, J. P., & Giosan, L. (2003). Wave-influenced deltas: Geomorphological implications for facies reconstruction. *Sedimentology*, 50(1), 187–210. <https://doi.org/10.1046/j.1365-3091.2003.00545.x>
- Bijkerk, J. F., Eggenhuisen, J. T., Kane, I. A., Meijer, N., Waters, C. N., Wignall, P. B., & McCaffrey, W. D. (2016). Fluvio-marine sediment partitioning as a function of basin water depth. *Journal of Sedimentary Research*, 86(3), 217–235. <https://doi.org/10.2110/jsr.2016.9>
- Brown, C. B. (1950). Sediment transportation. In H. Rouse (Ed.), *Engineering Hydraulics* (pp. 769–857). New York: John Wiley and Sons.
- Buckingham, E. (1914). On physically similar systems; illustrations of the use of dimensional equations. *Physical Review*, 4(4), 345–376. <https://doi.org/10.1103/PhysRev.4.345>
- Caldwell, R. L., Edmonds, D. A., Baumgardner, S., Paola, C., Roy, S., & Nienhuis, J. H. (2019). A global delta dataset and the environmental variables that predict delta formation. *Earth Surface Dynamics Discussion*, 2019, 1–26. <https://doi.org/10.5194/esurf-2019-12>
- Canicio, A., & Ibáñez, C. (1999). The Holocene evolution of the Ebre Delta Catalonia, Spain. *Acta Geographica Sinica*, 54(5), 462–469.
- Chadwick, A. J., Lamb, M. P., Moodie, A. J., Parker, G., & Nittrouer, J. A. (2019). Origin of a preferential avulsion node on Lowland River deltas. *Geophysical Research Letters*, 46, 4267–4277. <https://doi.org/10.1029/2019GL082491>
- Chatanantavet, P., Lamb, M. P., & Nittrouer, J. A. (2012). Backwater controls of avulsion location on deltas. *Geophysical Research Letters*, 39, L01402. <https://doi.org/10.1029/2011GL050197>
- Chawla, A., Spindler, D. M., & Tolman, H. L. (2013). Validation of a thirty year wave hindcast using the climate forecast system reanalysis winds. *Ocean Modelling*, 70, 189–206. <https://doi.org/10.1016/j.ocemod.2012.07.005>
- Chow, V. T. (1959). *Open-Channel Hydraulics* (Vol. 1). New York: McGraw-hill.
- Cooper, J. A. G. (1990). Ephemeral stream-mouth bars at flood-breach river mouths on a wave-dominated coast: Comparison with ebb-tidal deltas at barrier inlets. *Marine Geology*, 95(1), 57–70. [https://doi.org/10.1016/0025-3227\(90\)90021-B](https://doi.org/10.1016/0025-3227(90)90021-B)
- Dominguez, J. M. L. (1996). The Sao Francisco strandplain: A paradigm for wave-dominated deltas? *Geological Society, London, Special Publications*, 117(1), 217–231. <https://doi.org/10.1144/GSL.SP.1996.117.01.13>
- Edmonds, D. A., Hoyal, D. C. J. D., Sheets, B. A., & Slingerland, R. L. (2009). Predicting delta avulsions: Implications for coastal wetland restoration. *Geology*, 37(8), 759–762. <https://doi.org/10.1130/G25743A.1>
- Engelund, F., & Hansen, E. (1967). *A Monograph on Sediment Transport in Alluvial Streams*. Copenhagen, Denmark: Teknisk Forlag.
- Fisk, H. N. (1952). *Geological Investigation of the Atchafalaya Basin and the Problem of Mississippi River Diversion*. Vicksburg, MS: US Army Corps of Engineers.
- Ganti, V., Chadwick, A. J., Hassenruck-Gudipati, H. J., Fuller, B. M., & Lamb, M. P. (2016). Experimental river delta size set by multiple floods and backwater hydrodynamics. *Science Advances*, 2(5), e1501768. <https://doi.org/10.1126/sciadv.1501768>
- Ganti, V., Chu, Z., Lamb, M. P., Nittrouer, J. A., & Parker, G. (2014). Testing morphodynamic controls on the location and frequency of river avulsions on fans versus deltas: Huanghe (Yellow River), China. *Geophysical Research Letters*, 41, 7882–7890. <https://doi.org/10.1002/2014GL061918>
- Giosan, L., Syvitski, J., Constantinescu, S., & Day, J. (2014). Protect the world's deltas. *Nature*, 516(7529), 31–33. <https://doi.org/10.1038/516031a>
- Grijm, W. (1960). Theoretical forms of shorelines. *Paper Presented at the 7th Conference on Coastal Engineering, The Hague, The Netherlands* (Chap. 11, pp. 197–202). Lisbon, Portugal: ASCE. <https://doi.org/10.9753/icce.v7.11>
- Guillén, J., & Palanques, A. (1997). A historical perspective of the morphological evolution in the lower Ebro river. *Environmental Geology*, 30(3–4), 174–180. <https://doi.org/10.1007/s002540050144>
- Jansen, P. P., Van Bendegom, L., Van den Berg, J., De Vries, M., & Zanen, A. (1979). *Principles of River Engineering: The Non-Tidal Alluvial River*. London: Pitman.
- Jerolmack, D. J., & Swenson, J. B. (2007). Scaling relationships and evolution of distributary networks on wave-influenced deltas. *Geophysical Research Letters*, 34, L23402. <https://doi.org/10.1029/2007gl031823>
- Ma, H., Nittrouer, J. A., Naito, K., Fu, X., Zhang, Y., Moodie, A. J., et al. (2017). The exceptional sediment load of fine-grained dispersal systems: Example of the Yellow River, China. *Science Advances*, 3(5), e1603114. <https://doi.org/10.1126/sciadv.1603114>
- Ma, H., Nittrouer, J. A., Wu, B., Lamb, M. P., Zhang, Y., Mohrig, D., et al. (2020). Universal relation with regime transition for sediment transport in fine-grained rivers. *Proceedings of the National Academy of Sciences*, 117(1), 171–176. <https://doi.org/10.1073/pnas.1911225116>

- Mohrig, D., Heller, P. L., Paola, C., & Lyons, W. J. (2000). Interpreting avulsion process from ancient alluvial sequences: Guadalupe-Matarranya system (Northern Spain) and Wasatch formation (Western Colorado). *Bulletin of the Geological Society of America*, 112(12), 1787–1803. [https://doi.org/10.1130/0016-7606\(2000\)112<1787:IAPFAA>2.0.CO;2](https://doi.org/10.1130/0016-7606(2000)112<1787:IAPFAA>2.0.CO;2)
- Moodie, A. J., Nittrouer, J. A., Ma, H., Carlson, B. N., Chadwick, A. J., Lamb, M. P., & Parker, G. (2019). Modeling deltaic lobe-building cycles and channel avulsions for the Yellow River Delta, China. *Journal of Geophysical Research: Earth Surface*, 124, 2438–2462. <https://doi.org/10.1029/2019jf005220>
- Muto, T., & Swenson, J. B. (2005). Large-scale fluvial grade as a nonequilibrium state in linked depositional systems: Theory and experiment. *Journal of Geophysical Research*, 110, F03002. <https://doi.org/10.1029/2005jf000284>
- Nienhuis, J. H., Ashton, A. D., Edmonds, D. A., Hoitink, A. J. F., Kettner, A. J., Rowland, J. C., & Törnqvist, T. E. (2020). Global-scale human impact on delta morphology has led to net land area gain. *Nature*, 577(7791), 514–518. <https://doi.org/10.1038/s41586-019-1905-9>
- Nienhuis, J. H., Ashton, A. D., & Giosan, L. (2015). What makes a delta wave-dominated? *Geology*, 43(6), 511–514. <https://doi.org/10.1130/G36518.1>
- Nienhuis, J. H., Ashton, A. D., & Giosan, L. (2016). Littoral steering of deltaic channels. *Earth and Planetary Science Letters*, 453, 204–214. <https://doi.org/10.1016/j.epsl.2016.08.018>
- Nienhuis, J. H., Ashton, A. D., Kettner, A. J., & Giosan, L. (2017). Large-scale coastal and fluvial models constrain the late Holocene evolution of the Ebro Delta. *Earth Surface Dynamics*, 5(3), 585–603. <https://doi.org/10.5194/esurf-5-585-2017>
- Nienhuis, J. H., Ashton, A. D., Nardin, W., Fagherazzi, S., & Giosan, L. (2016). Alongshore sediment bypassing as a control on river mouth morphodynamics. *Journal of Geophysical Research: Earth Surface*, 121(4), 664–683. <https://doi.org/10.1002/2015JF003780>
- Nienhuis, J. H., Törnqvist, T. E., & Esposito, C. R. (2018). Crevasse splays versus avulsions: A recipe for land building with levee breaches. *Geophysical Research Letters*, 45, 4058–4067. <https://doi.org/10.1029/2018GL077933>
- Paola, C., & Mohrig, D. (1996). Palaeohydraulics revisited: Palaeoslope estimation in coarse-grained braided rivers. *Basin Research*, 8(3), 243–254. <https://doi.org/10.1046/j.1365-2117.1996.00253.x>
- Paola, C., & Voller, V. R. (2005). A generalized Exner equation for sediment mass balance. *Journal of Geophysical Research*, 110, F04014. <https://doi.org/10.1029/2004JF000274>
- Ratliff, K. M., Hutton, E. H. W., & Murray, A. B. (2018). Exploring wave and sea-level rise effects on delta morphodynamics with a coupled river-ocean model. *Journal of Geophysical Research: Earth Surface*, 123, 2887–2900. <https://doi.org/10.1029/2018JF004757>
- Rodriguez, A. B., Hamilton, M. D., & Anderson, J. B. (2000). Facies and evolution of the modern Brazos Delta, Texas: Wave versus flood influence. *Journal of Sedimentary Research*, 70(2), 283–295. <https://doi.org/10.1306/2DC40911-0E47-11D7-8643000102C1865D>
- Smith, N. D., Cross, T. A., Dufficy, J. P., & Clough, S. R. (1989). Anatomy of an avulsion. *Sedimentology*, 36(1), 1–23. <https://doi.org/10.1111/j.1365-3091.1989.tb00817.x>
- Sonin, A. A. (2004). A generalization of the Π -theorem and dimensional analysis. *Proceedings of the National Academy of Sciences of the United States of America*, 101(23), 8525–8526. <https://doi.org/10.1073/pnas.0402931101>
- Swenson, J. B. (2005). Relative importance of fluvial input and wave energy in controlling the timescale for distributary-channel avulsion. *Geophysical Research Letters*, 32, L23404. <https://doi.org/10.1029/2005gl024758>
- Svititski, J. P. M., Kettner, A. J., Overeem, I., Hutton, E. W. H., Hannon, M. T., Brakenridge, G. R., et al. (2009). Sinking deltas due to human activities. *Nature Geoscience*, 2(10), 681–686. <https://doi.org/10.1038/ngeo629>
- Wang, J., Muto, T., Urata, K., Sato, T., & Naruse, H. (2019). Morphodynamics of river deltas in response to different basin water depths: An experimental examination of the grade index model. *Geophysical Research Letters*, 46, 5265–5273. <https://doi.org/10.1029/2019gl082483>
- Wang, Z. B., Wang, Z. Y., & de Vriend, H. J. (2008). Impact of water diversion on the morphological development of the lower Yellow River. *International Journal of Sediment Research*, 23(1), 13–27. [https://doi.org/10.1016/S1001-6279\(08\)60002-5](https://doi.org/10.1016/S1001-6279(08)60002-5)
- Wang, Z. Y., & Liang, Z. Y. (2000). Dynamic characteristics of the Yellow River mouth. *Earth Surface Processes and Landforms*, 25(7), 765–782. [https://doi.org/10.1002/1096-9837\(200007\)25:7<765::AID-ESP98>3.0.CO;2-K](https://doi.org/10.1002/1096-9837(200007)25:7<765::AID-ESP98>3.0.CO;2-K)
- Zenkovich, V. P. (1967). In J. A. Steers, & C. A. M. King (Eds.), *Processes of Coastal Development*. New York: Interscience (Wiley).
- Zheng, S., Han, S., Tan, G., Xia, J., Wu, B., Wang, K., & Edmonds, D. A. (2018). Morphological adjustment of the Qingshuigou channel on the Yellow River Delta and factors controlling its avulsion. *Catena*, 166, 44–55. <https://doi.org/10.1016/j.catena.2018.03.009>
- Zheng, S., Wu, B., Wang, K., Tan, G., Han, S., & Thorne, C. R. (2017). Evolution of the Yellow River delta, China: Impacts of channel avulsion and progradation. *International Journal of Sediment Research*, 32(1), 34–44. <https://doi.org/10.1016/j.ijsrc.2016.10.001>